

Article

Acidification and Deoxygenation of the Northwestern Japan/East Sea

Pavel Tishchenko *, Vyacheslav Lobanov , Dmitry Kaplunenko , Sergey Sagalaev and Petr Tishchenko 

V.I. Il'ichev Pacific Oceanological Institute, Far Eastern Branch, Russian Academy of Sciences, 690041 Vladivostok, Russia; lobanov@poi.dvo.ru (V.L.); dimkap@poi.dvo.ru (D.K.); sagalaev@poi.dvo.ru (S.S.); eq15@poi.dvo.ru (P.T.)
* Correspondence: tpavel@poi.dvo.ru; Tel.: +7-423-231-3092

Abstract: Seasonal hypoxia in the bottom waters of the Peter the Great Bay (PGB) of the Japan/East Sea (JES) occurs in summer. Using the empirical relationship between dissolved oxygen (DO) and pH obtained for hypoxic conditions and available historical DO data, acidification rates were estimated. Carefully sampled time-series observations from the northwestern part of the JES, carried out from 1999 to 2014 along the 132°20' E and 134°00' E longitudes, were chosen to determine the interannual variability of the sea's hydrochemical parameters (DO, pH, and TA—the total alkalinity phosphates, nitrate, and silicates). To limit the effects of seasonal and spatial variability, only data obtained in the warm period were used. Additionally, all data from depths shallower than 500 m were discarded because they are affected by high natural variability, mostly due to strong mesoscale dynamic structures. Our results demonstrated that the pH and DO concentrations measured in the Upper Japan Sea Proper Water (750 m), Lower Japan Sea Proper Water (1250, 1750, 2250 m), and Bottom Water (3000 m) have been decreasing in recent years. On the other hand, calculated normalized dissolved inorganic carbon (NDIC), CO₂ partial pressure (pCO₂), and measured nutrient concentrations have been increasing. Maximum rates of acidification and deoxygenation are occurring at around 750 m. The annual rate of increase of pCO₂ in the water exceeds the atmospheric rate more than 2-fold at a depth of 750 m. The observed variability of the hydrochemical properties can be explained by the combination of the slowdown ventilation of the vertical water column and eutrophication. However, the results obtained here are valid for the subpolar region of the JES, not for the whole sea. The synchronization of the deoxygenation of the open part of the JES and PGB has been found.



Citation: Tishchenko, P.; Lobanov, V.; Kaplunenko, D.; Sagalaev, S.; Tishchenko, P. Acidification and Deoxygenation of the Northwestern Japan/East Sea. *J. Mar. Sci. Eng.* **2021**, *9*, 953. <https://doi.org/10.3390/jmse9090953>

Academic Editor: Maria Gabriella Marin

Keywords: acidification; deoxygenation; eutrophication; Japan/East Sea; Peter the Great Bay

Received: 17 July 2021

Accepted: 28 August 2021

Published: 1 September 2021

Publisher's Note: MDPI stays neutral with regard to jurisdictional claims in published maps and institutional affiliations.



Copyright: © 2021 by the authors. Licensee MDPI, Basel, Switzerland. This article is an open access article distributed under the terms and conditions of the Creative Commons Attribution (CC BY) license (<https://creativecommons.org/licenses/by/4.0/>).

1. Introduction

The Japan/East Sea (JES) is a semi-enclosed marginal sea of the western North Pacific (Figure 1). An important feature of the JES is the Subpolar Front, which is a zonal current crossing the JES at about 40° N. The Subpolar Front divides the JES into subtropical and subpolar regimes [1]. JES is very well ventilated at all depths. The dissolved oxygen (DO) concentration in the JES is higher than anywhere else in the Pacific due to deep ventilation [1,2]. However, there are published papers that suggest that the interior of the JES is currently undergoing deoxygenation and acidification (lowering the pH over time). Gamo et al. [3] were the first to detect an ongoing decline in DO concentrations in the JES. Since then, many scientists have clearly demonstrated that the interior of the JES has undergone drastic changes over the last 60 years, including continuous warming and a significant decrease in DO in deep waters [4–11]. There is strong experimental evidence of acidification of the JES [12–14]. Using experimental data on total alkalinity (TA), pH, and dissolved inorganic carbon (DIC), obtained in 1992, 1999, and 2007 for depths of 50–1000 m, Kim et al. [12] estimated the effect of anthropogenic CO₂ on the aragonite saturation horizon ($\Omega_{\text{arag}} = 1$). The anthropogenic CO₂ accumulation in the JES from 1800 to 1999 has displaced the $\Omega_{\text{arag}} = 1$ depth upward by 50–250 m in locations across the basin [12]. The

authors of [12,13] assumed that anthropogenic carbon is responsible for the acidification of the JES. Chen et al. [14], using a model of respiration of organic matter, estimated that the acidification rate near the bottom of the JES is 27% higher than at the surface as a result of the increasing CO₂ partial pressure (pCO₂) in the atmosphere. The authors explained this phenomenon by the reduced ventilation of the sea due to global warming.

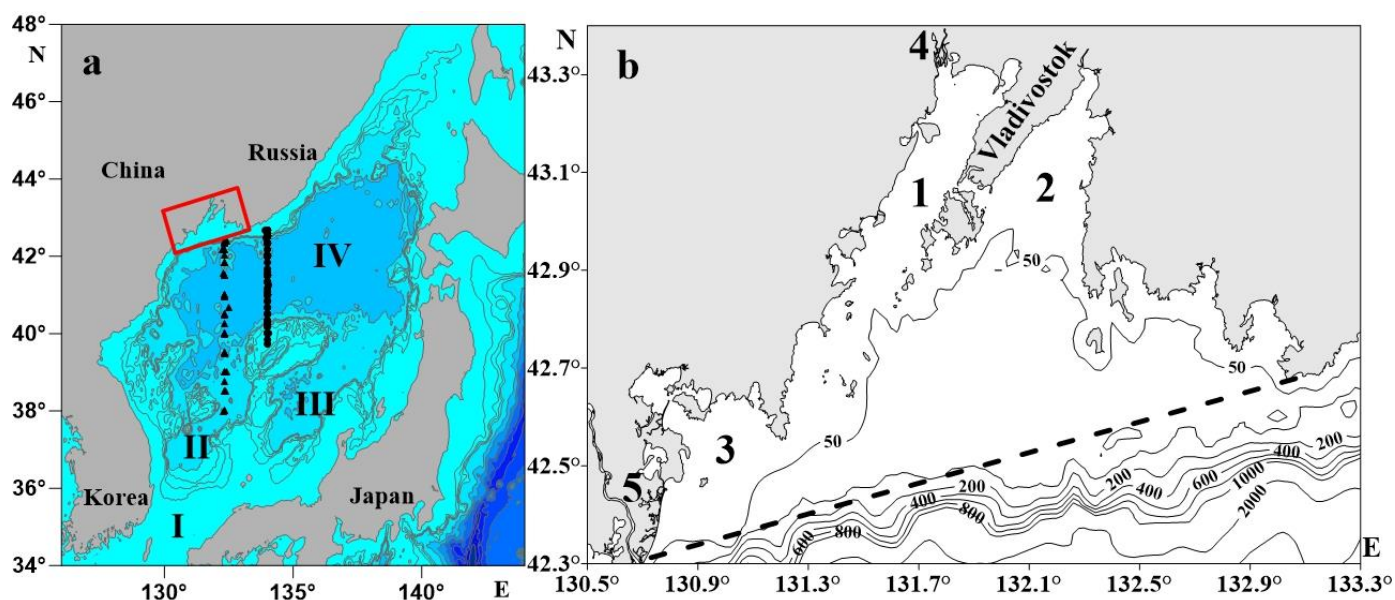


Figure 1. (a) Map of the Japan/East Sea (JES), I—Tsushima (Korean) Strait, II—Ulleung, III—Yamato; and IV—Japan deep basins; station locations along 132°20' E are shown by triangles and along 134°00' E by circles; the red rectangle shows PGB. (b) Map of Peter the Great Bay (PGB); 1, 2, 3—Amursky, Ussuriysky, and Posyet Bays, respectively; 4, 5—Razdolnaya and Tumannaya Rivers, respectively. The dashed line indicates the border of PGB.

The Peter the Great Bay (PGB), located on the northwestern shelf of the JES (Figure 1b), reveals seasonal hypoxia [15]. It has been established that the nutrients supplied by the Razdolnaya Bay and Tumannaya River cause eutrophication and induce seasonal hypoxia in its bottom waters. Amursky Bay is a secondary bay of the PGB that regularly demonstrates hypoxic events in the bottom water in late summer [16]. Hydrochemical observations (DO, phosphorus, silica, pH, DIC, and ammonium) suggest that the main cause of hypoxia is the degradation of “excess” diatoms at the water/bottom sediment interface under slow water dynamic conditions. Available historical data clearly demonstrate that the lowest values of DO obtained in the summer at the bottom waters of Amursky Bay have been steadily decreasing over the last 80 years (Figure 2; [17]).

Using our experimental data, we demonstrate below that acidification, deoxygenation, and increasing nutrient concentrations in the interior of the northwestern JES (below 500 m) are a result of a nonstationary process of the aerobic degradation of organic matter. The rates of acidification and deoxygenation of the water column can be explained by two mechanisms. One of them is a slowdown of the ventilation of the water column (currently the generally accepted point of view). The other is the eutrophication of the northwestern part of the JES (this point of view was first presented by Gamo et al. [3]). However, the observed deoxygenation and estimated acidification on the shelf of the JES (PGB) are mostly caused by the eutrophication of coastal waters due to the supply of nutrients by eutrophic transboundary Razdolnaya and Tumannaya Rivers, which flow into Amursky Bay and the southwestern part of PGB, respectively (Figure 1b). There is a synchronization between the deoxygenation of the open part of the JES and the formation of hypoxia in the bottom waters of PGB, as discussed below. Due to the existence of a Subpolar Front that divides the JES into subtropical and subpolar regimes, the results obtained here are valid for the subpolar region of the JES, not for the whole sea.

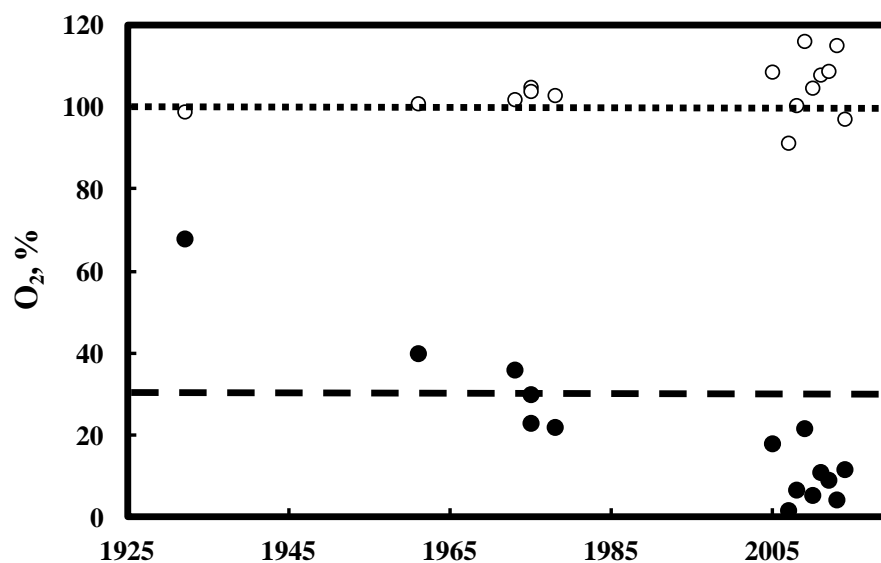


Figure 2. Interannual variability of minimal values of DO concentrations (saturation degree) observed in the bottom waters of Amursky Bay in the summer (filled circles) and corresponding values for surface waters (open circles) [17]. The dashed line corresponds to hypoxia, while the dotted line corresponds to 100% saturation.

2. Materials and Methods

2.1. Dataset

Data were collected at 99 stations in Amursky Bay (Figure 1b) on 14–28 August 2007. Water samples were taken from the surface and bottom layers using 10-L Niskin bottles. The bottom sample was taken at a depth of 1.0–1.5 m above the sea floor, while the surface sample was taken from a depth of 1.0–1.5 m below the surface. The samples were immediately analyzed to obtain the following parameters: salinity, DO, pH, TA, and nutrients (silica, phosphorus, nitrates, nitrites, and ammonium). Vertical profiles of the temperature, salinity, and turbidity were measured with a Sea-Bird 19plus CTD profiler at each station [16]. During the survey, severe hypoxia was found in the bottom waters [18]. There are nutrient and discharge data available for the Razdolnaya and Tumannaya Rivers [15,19] (Primorskiy Administration of Russian Hydrometeorological Service (<https://gmvo.skniivh.ru/index.php?id1/41>) (Data were accessed on 1 July 2018). These data made it possible to assess the temporal trend of annual nutrient fluxes into Amursky Bay and the JES in 2003–2017.

In the open sea, since 1999, quite intensive fieldwork has been completed through international collaboration, including more than 20 cruises undertaking hydrochemical surveys of the northwestern part of the JES in different seasons. These surveys have been implemented under the Circulation Research of the East Asian Marginal Seas (CREAMS) program, including the CREAMS-II international program in 1999–2001, followed by the joint research of the V.I. Il'ichev Pacific Oceanological Institute (POI) (Russia) and Seoul National University (Korea). Two meridional sections (132°20' E and 134°00' E) were chosen to be sampled over the period 1999–2014. The metadata are presented in Table 1. Most stations were located north of 40° N; only four were located between 40° and 38° N (Figure 1).

Table 1. Metadata of hydrochemical observations along meridional sections 132°20' E and 134°00' E in 1999–2014.

R/V	Cruise	Month	Year	Number of Stations
<i>Roger Revelle</i>	HNRO7	June–July	1999	7
<i>Professor Khromov</i>	Kh36	July–August	1999	16
<i>Professor Gagarinskiy</i>	Ga31a	April	2001	11
<i>Professor Gagarinskiy</i>	Ga31b	May–June	2001	11
<i>Akademik M.A. Lavrentyev</i>	La33	May	2004	10
<i>Akademik M.A. Lavrentyev</i>	La35	March	2005	6
<i>Professor Gagarinskiy</i>	Ga43	May	2007	13
<i>Akademik M.A. Lavrentyev</i>	La46	July	2009	10
<i>Professor Gagarinskiy</i>	Ga47	May	2010	5
<i>Akademik M.A. Lavrentyev</i>	La66	April	2014	16

The seasonal variability of the hydrochemical parameters in the northern part of the sea is very strong [2,20]. For this reason, only data obtained in the warm period were used in our analysis. Mesoscale water dynamics cause high spatial and temporal variability of the hydrochemical parameters, especially in the upper 500 m, as can be seen from the distributions of DO concentration and pH in Figure 3. We therefore excluded data of the upper 500 m layer from further analysis.

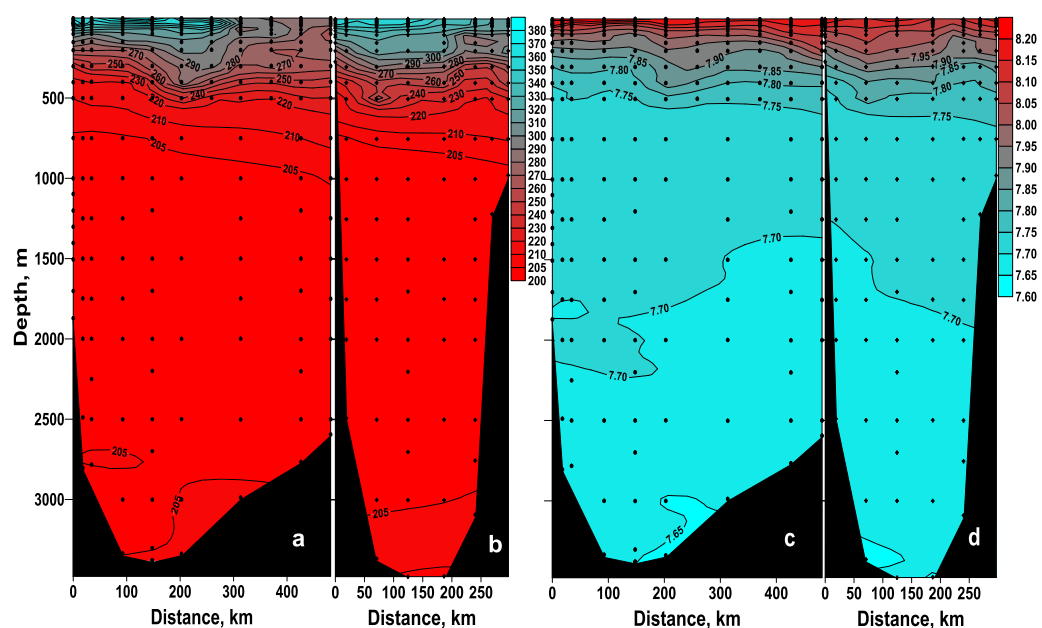


Figure 3. Meridional sections of dissolved oxygen concentrations (a,b) and pH_{in situ} (c,d) along 132°20' E (a,c) and 134°00' E (b,d), April 2014.

2.2. Analytical Methods

Hydrochemical parameters (DO, pH_T, TA, phosphorus, silica, and nitrate) in the northwestern part of the JES were measured using methods described elsewhere [21]. All hydrochemical parameters were analyzed on board the ship as soon as possible after sampling by Niskin bottle. Nutrients were determined by the photometrical method. Uncertainties in the nutrient data were about ±2% at the studied concentrations. Details of the methods used for nutrient analysis are given in [22]. In 2012, the POI participated in the intercalibration of nutrient measurements, carried out by Prof Aoyama. The results of the intercalibration are presented in the Supplementary Materials. Our data show good agreement with the data of other laboratories (Figures S1–S5). DO samples were analyzed using an automated oxygen titrator with a Brinkman Dosimat burette and photometric end-point detection. Details of the Winkler titration method, providing accuracy of the

measurements of 0.5 to 1%, are described in [21]. Samples for pH referenced to 15 °C were measured by a cell without a liquid junction. Details of this method, providing accuracy of ± 0.004 pH units, are given in [23]. The measured pH values are given on the total hydrogen concentration scale [23]. The main body of proper waters of the JES is very uniform in terms of its hydrochemical characteristics, and our vertical profiles of pH presented in Figures S6 and S7 suggest good precision and accuracy (the data presented in Figure S7 were obtained on different cruises by different operators and different equipment).

The analysis of TA used direct colorimetric titration with hydrochloric acid in an open system using a mixed indicator (methylene blue and methyl red). The titration was carried out in CO₂-free conditions via the flow of CO₂-free air (or nitrogen). Calibration of the HCl was carried out using Dickson’s Certified Reference Materials. This method is known as Bruevich’s method [21] and gives an accuracy of $\pm 0.15\%$. To remove the effects of evaporation and precipitation, as well as mixing and upwelling processes, normalized TA (NTA) ($NTA = 35 \cdot TA/S$) was used in the analysis rather than TA. In the expeditions on R/V *RogerRevelle* and *Professor Khromov* (1999), the procedure of TA measurements included daily control of our system by calibration of acid using Dickson’s CRM standard. Therefore, the alkalinity data of this cruise were accepted as a reference. Averaged differences of NTA between particular cruises and the 1999 cruises ($\Delta NTA = NTA(\text{year}) - NTA(1999)$) showed no noticeable temporal variability (Figure 4). Therefore, it was accepted that the NTA of the JES does not have any temporal variability and equals the NTA obtained in 1999 on R/Vs *RogerRevelle* and *Professor Khromov*. Therefore, the TA values for a given year were corrected with reference to the TA obtained in 1999. Corrected TA data for the given years, as well as measured pH and CTD data, were used for the calculation of the carbonate system parameters (DIC, $pH_{in situ}$, and pCO_2).

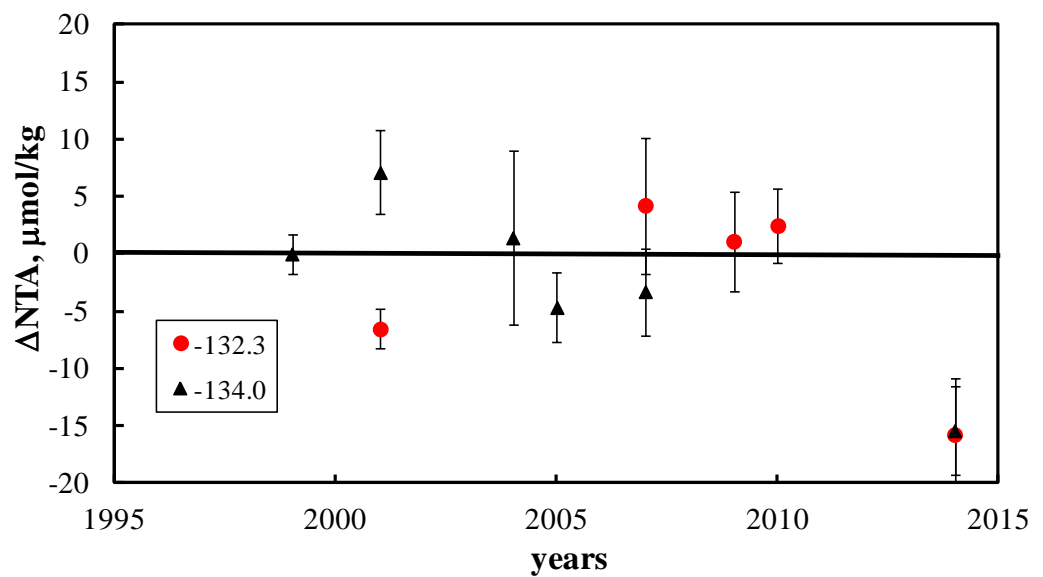


Figure 4. Averaged differences of NTA between particular cruises (given year cruises) and 1999 cruises ($\Delta NTA = NTA(\text{year}) - NTA(1999)$). Water samples were taken along 132°20' E (red) and 134°00' E (black) sections. Bars are 3·s.d. = 3·[s.d.(year + s.d.(1999))].

2.3. Data Processing

The eutrophication of PGB produces excessive organic matter degradation (OM), which leads not only to hypoxic conditions in the bottom waters, but also to a decrease in the pH. The same respiratory process consumes DO and releases carbon dioxide. Using the measured pH and TA data for the bottom waters of Amursky Bay, $pH_{in\ situ}$ values were calculated for August 2007 and presented as a function of the DO concentration in Figure 5a. The line in this figure was calculated using the following empirical relationship:

$$pH_T(\text{in situ}) = 7.349 + 9.436 \cdot 10^{-3} [O_2] - 2.364 \cdot 10^{-5} [O_2]^2, \quad (1)$$

with $R^2 = 0.95$, where $[O_2]$ is the measured concentration of DO (saturation degree, %); pH_T is the pH on the total hydrogen concentration scale [24]. Equation (1) was obtained with the LSM ($r^2 = 0.95$). It should be noted that the link between DO and pH has been previously used for modeling respiration/acidification processes in acidification [14,25,26]. Equation (1) and the available historical oxygen data (Figure 2) provide the interannual variability in the $pH_{in\ situ}$ of the bottom waters of Amursky Bay caused by eutrophication (Figure 5b).

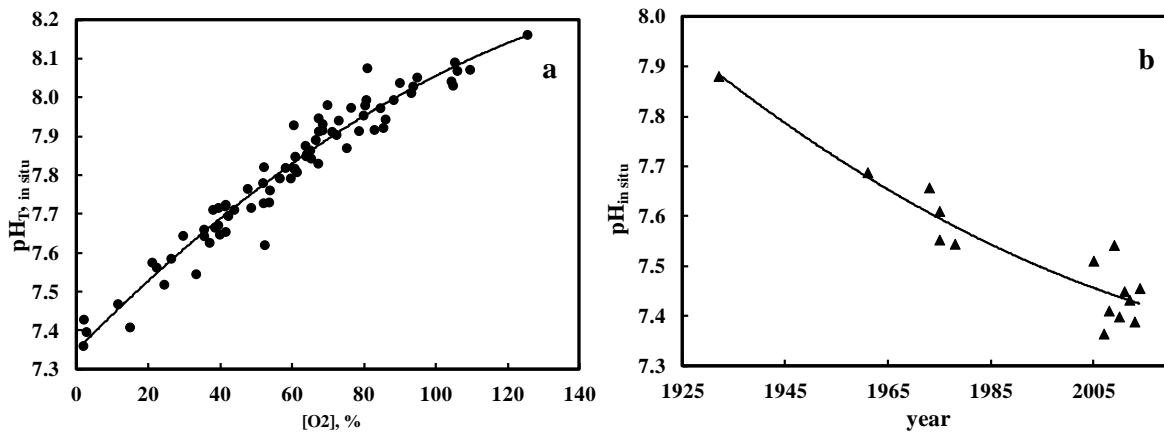


Figure 5. Dependence of (a) pH_T (in situ) vs. DO saturation degree; (b) interannual variability of $pH_{in\ situ}$ values in the bottom waters of Amursky Bay in summer, predicted by Equation (1).

Daily nutrient fluxes, J_i , were estimated from the available concentrations of nutrients in the river waters, C_i [15,19], and available water discharges, Q_R , of the Razdolnaya River using the following equation:

$$J_i = Q_R \cdot C_i. \quad (2)$$

The water discharge of the Tumannaya River, Q_T , was estimated using available data of Q_R and the empirical relationship [15]:

$$Q_T = a \cdot Q_R^b, \quad (3)$$

where $a = 0.775$, $b = 1.264$. Annual fluxes of nutrients, F_i , were estimated by means of the following equation:

$$F_i = \sum_n J_i(n), \quad (4)$$

where n is the number of days in a year.

In the open sea, for each year, all data were grouped into five depth intervals: 500–1000 m, 1000–1500 m, 1500–2000 m, 2000–2500 m, and 2500–3400 m (or bottom). Within each group, for a given year, the original hydrochemical parameters were calculated for nominal depths (750, 1250, 1750, 2250, and 3000 m) using the empirical dependences of given parameters as functions of depth. These empirical dependences were obtained by the Least Squares Method (LSM). Then, each value, corrected for nominal depth, was used for estimation of temporal variability by means of the LSM method. All statistical tests were

performed using the statistical software Microsoft Excel, Moscow, Russia. A regression analysis (i.e., LSM) was performed to obtain the empirical relationships. Statistical tests were characterized by the standard deviation (s.d.) with a 95% confidence interval (i.e., $p < 0.05$). Linear regression of dependences, as shown in Figures 6 and 7, was used for estimation of the rate of variability (and its s.d.) of each hydrochemical parameter. The estimated error of the rate of variability was accepted as 3-s.d. Details about our data are given in Tables S1 and S2. These are average values of the measured parameters for each nominal depth, the number of original measurements used for the calculation of the average values, and the standard deviation of the mean ($3s.d. (\text{mean}) = 3s.d./\sqrt{n}$).

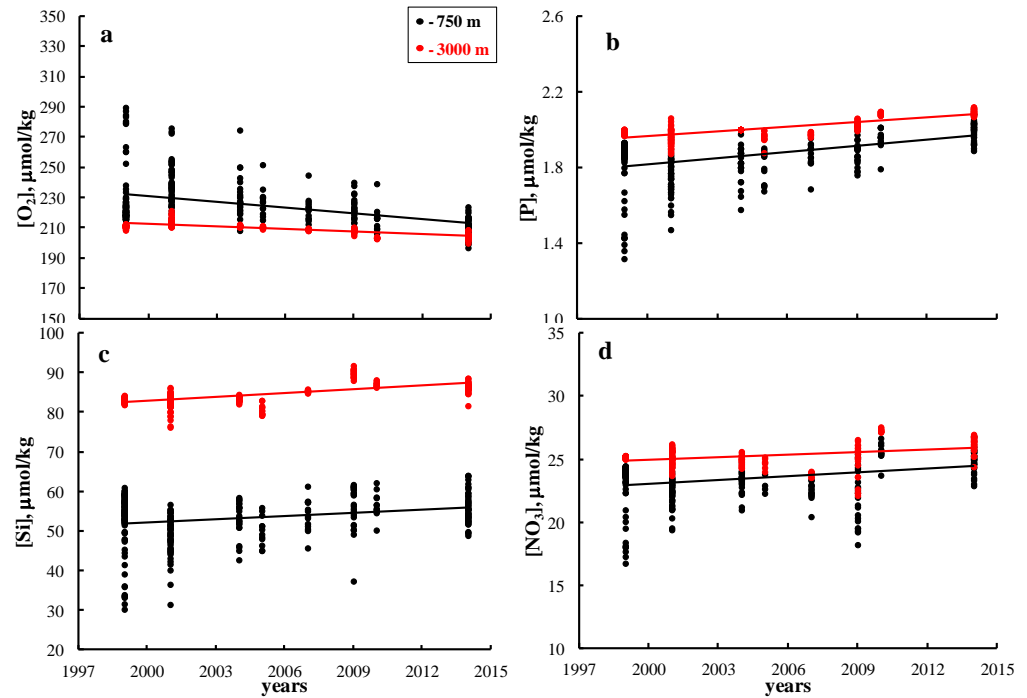


Figure 6. Temporal variability of the hydrochemical parameters in the JES at 750 m (black) and 3000 m (red) depths. (a) DO concentrations (µmol/kg); (b) phosphorus concentrations (µmol/kg); (c) silica concentrations (µmol/kg); (d) nitrate concentrations (µmol/kg).

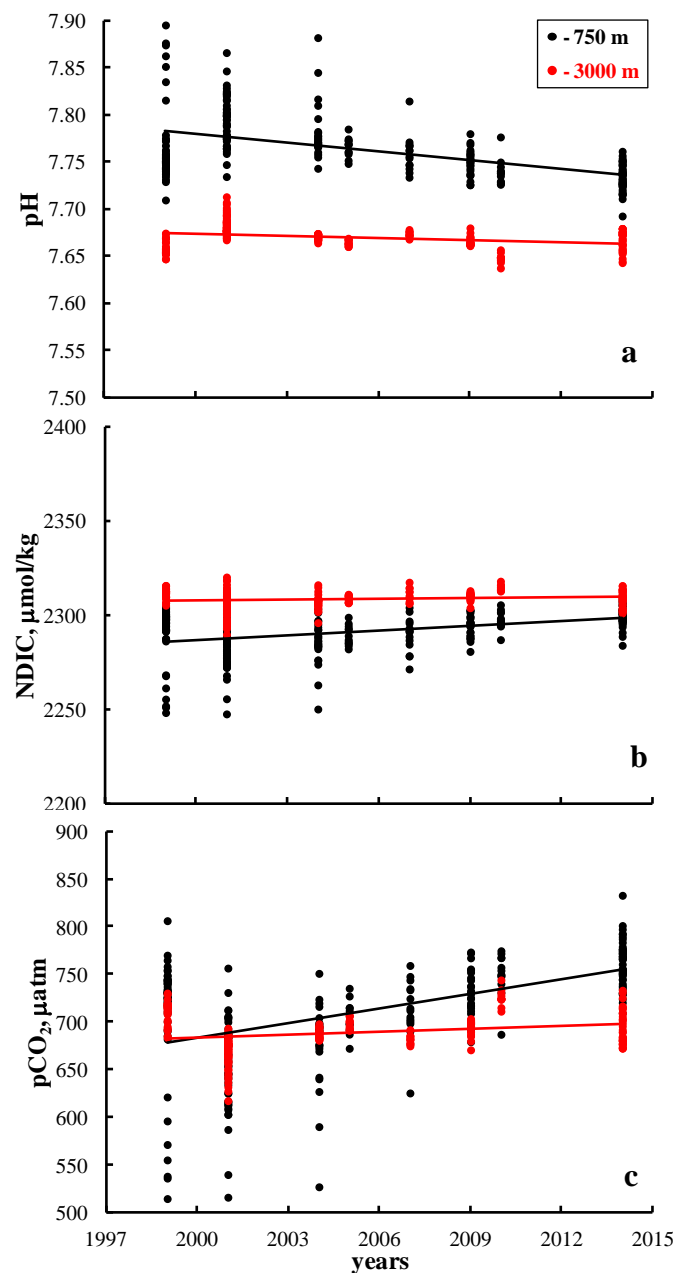


Figure 7. Temporal variability of the carbonate system parameters in the JES at 750 m (black) and 3000 m (red) depths. (a) pH (in situ); (b) Normalized Dissolved Inorganic Carbon (NDIC = DIC·35/S); (c) carbon dioxide partial pressure.

3. Results and Discussion

The PGB is situated in the northwestern part of the JES (Figure 1). Based on the detailed hydrological and hydrochemical surveys carried out during 2007–2016, a seasonal hypoxia event was discovered in four places in the PGB: (1) a central area of the Amursky Bay, where hypoxia was observed in August 2007 [15,18]; (2) the Far East Marine Biosphere Reserve (Posyet Bay), where hypoxia was discovered in August 2013 [15,27]; (3) an internal part of the Razdolnaya River estuary, where hypoxia was observed in October 2014 [28]; and (4) an internal part of the Tumannaya River estuary, where hypoxia was observed in May 2015 [29]. The Tumannaya and Razdolnaya Rivers are transboundary rivers that originate in China.

Amursky Bay is a secondary bay of the PGB that regularly demonstrates hypoxic events in the bottom water in the late summer [16]. Available historical data clearly

demonstrate that the lowest values of DO obtained in the summer in the bottom waters of Amursky Bay have been steadily decreasing over the last 80 years (Figure 2; [17]). The slope of the solid line in Figure 5b indicates summer acidifications of the bottom waters on the shelf of the JES caused by OM respiration, which varies from -0.0080 pH units/y (1932) to -0.0033 pH units/y (2014). According to the pH vs. $[O_2]$ ratio (Figure 5a), one should expect an increase in the acidification rate with decreasing DO. However, the nonlinearity of the solid line in Figure 5b indicates decreasing acidification over time. That is mostly caused by the decrease in the deoxygenation rate over time (Figure 1). Obviously, there is a limit to the DO concentration near the bottom, i.e., 0. In 2007 and 2011, the DO saturation degree was 1.7 and 4.3, respectively. Additionally, it should be noted that under limited oxygen conditions (hypoxia), the rate of microbial oxidation of OM at the water/bottom sediment interface is low, because this reaction is of the first order [17].

Using available data and Equations (2)–(4), annual nutrient fluxes (DIN—dissolved inorganic nitrogen, DIP—dissolved inorganic phosphorus, Si—silica) and DOC (dissolved organic carbon) were estimated for 2003–2017. The results are presented in Figure 8.

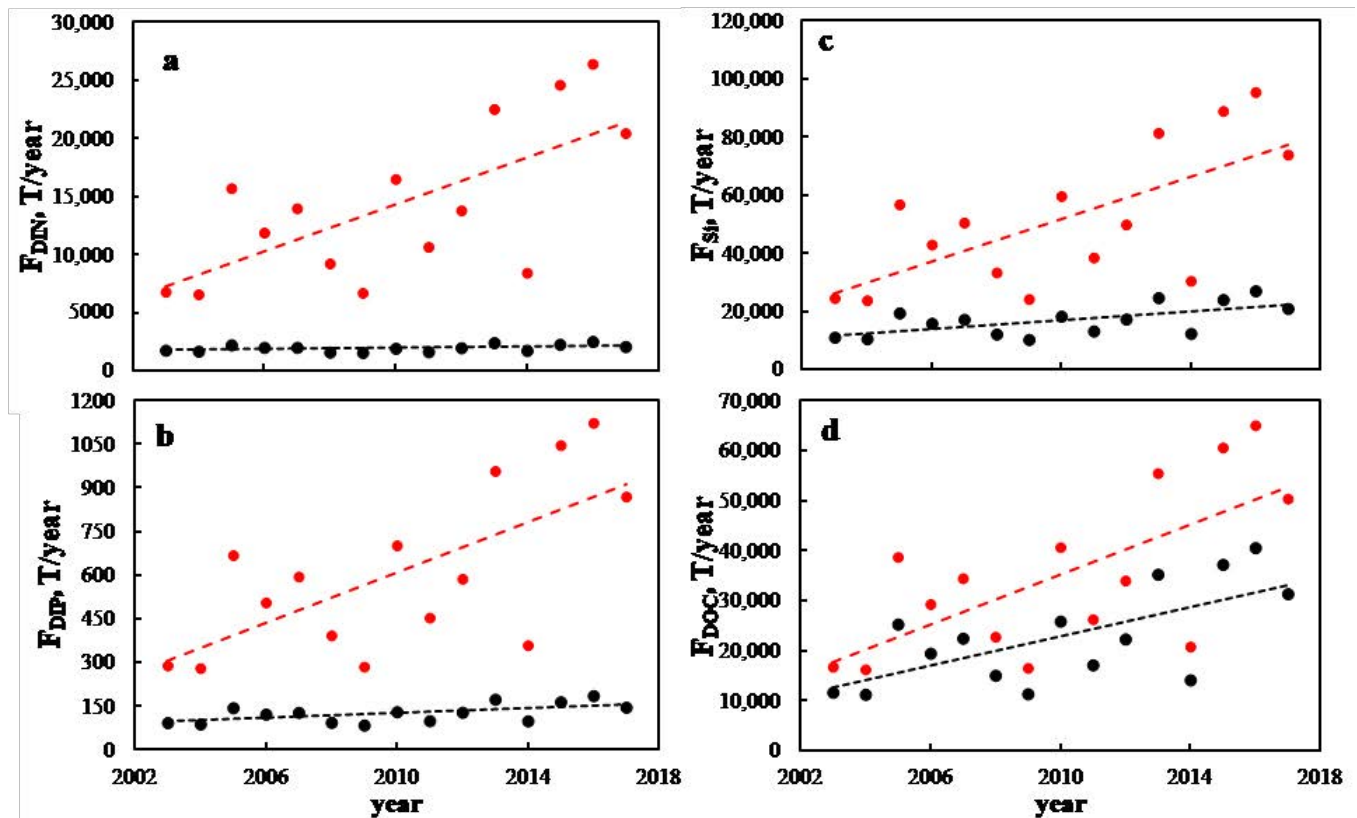


Figure 8. Annual fluxes of (a) DIN, (b) DIP, (c) silica, (d) DOC supplied by the Razdolnaya River into Amursky Bay (black circles) and by the Tumannaya River into the JES (red circles) in 2003–2017.

River waters have high nutrient concentrations. On average, there are, 1.8, 75, and 230 and 2.2, 116, and 210 $\mu\text{mol}/\text{kg}$ of DIP, DIN, and silica, respectively, in the Razdolnaya and Tumannaya Rivers. Concentrations of nutrients tend to increase in Razdolnaya River over time [30]. Due to the increase in river water discharge over time, Figure 8 demonstrates the increasing annual fluxes of nutrients in 2003–2017. This means that eutrophication of the northwestern part of the JES occurred.

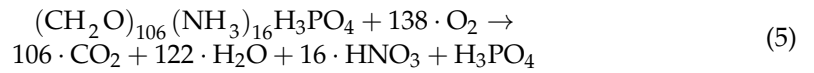
The long-term biological and DO observations in Amursky Bay are consistent with one another: maximal changes in the composition and structure of bottom fauna in Amursky Bay occurred at the same time in the 1970s–1980s, when the minimum DO values declined to a hypoxic state (Figure 2) [31–33]. In this period, eutrophication-tolerant animals such as Polychaeta, Bivalvia, and Amphipoda, which had previously been observed just occa-

sionally, became common species in the bay and had maximal abundance [34]. Most of the authors attributed these observed changes in the species structure of benthos in the bay to chronic human pollution and eutrophication [32–34]. It is also likely that acidification may negatively affect the zoobenthos in the bay. However, it is difficult to distinguish between the effects of low oxygen, H₂S production, and acidification on biota.

In the open JES, below the main thermocline, there is a large uniform water mass known as the Japan Sea Proper Water [35]. Due to the small variations in salinity and temperature and their time dependence throughout the water column, water-mass definitions based on specific property ranges are not particularly useful [1]. Nevertheless, using definitions of the JES water masses [1], nominal depths of 750 m; 1250, 1750, and 2250 m; and 3000 m can be assigned to the Upper Japan Sea Proper Water, Lower Japan Sea Proper Water, and Bottom Water, respectively. The decadal variability of hydrochemical parameters (DO, phosphates, nitrates, and silicates) and parameters of the carbonate system (pH_{in situ}, NDIC, pCO₂) for depths of 750 and 3000 m in the JES are presented in Figures 6 and 7. The estimated errors of each measured parameter due to the method of chemical analysis are much less than the scattering around the dependences illustrated in Figures 9 and 10. This means that there are natural processes, such as water dynamics (Figure 3), that increase the scatter around the secular variability of the hydrochemical parameters, especially at 750 m (Figures 9 and 10). The scattering amplitude is apparently decreasing over time. Probably, this is a result of the slowdown of intensity of mesoscale eddies that were crossed by our meridional sections along 132°20' and 134° E during the implementation of the surveys (Figure 1). Our data demonstrate that the pH and DO concentrations in Upper Japan Sea Proper Water, Lower Japan Sea Proper Water, and Bottom Water masses have decreased over time. An opposite tendency was seen for nutrients (phosphorus, silica, and nitrates), NDIC, and pCO₂. The rates of variability as a function of depth are shown in Figures 9 and 10. The rates of oxygen concentration declining in the interior of the JES agrees with previous publications [3–11,14]. Moreover, the deoxygenation rates for depths of 2000–3000 m, estimated as 10% per 30 years (0.67 μmol/(kg·year)) by Gamo et al. [36], and (0.66–0.68 μmol/(kg·year)) by Chen et al. [14], are in good agreement with our results (Figure 9). The acidification rate is –0.003 pH unit/year in the Upper Japan Sea Proper Water (750 m). The estimated acidification rate at 500 m was –0.004 pH unit/year [14], which is in good agreement.

According to Henry's law, the increase in CO₂ of the atmosphere will increase its concentration in the mixed layer of the ocean and thus decrease the pH of surface waters. In fact, there is direct published evidence of a significant long-term decrease in surface pH. The expected rate of decrease in pH has been estimated as –0.0017 units pH/year, based on the rate of CO₂ increase in the atmosphere [37–41]. This acidification of the ocean is driven by increasing atmospheric CO₂, which mostly results from fossil fuel combustion, the manufacturing of cement, and deforestation. However, in some cases, the observed acidification rates of surface waters are even higher than the estimated ones. For example, –0.0024 units pH/year has been observed in the Iceland Sea [42] and –0.0030 units pH/year in the JES [13]. Generally, the ocean acidification signal becomes weaker with depth [37,40,42]. However, in some subsurface layers, between 150 and 400 m, acidification rates as high as –0.0040 units pH/year have been reported in the North Pacific Ocean [39]. There are other drivers that can increase the acidification of seawater, such as slowed-down water column ventilation by vertical mixing and an increase in respiration rates due to eutrophication and acidic rains [39,43–45]. These drivers link the acidification and deoxygenation processes in the subsurface and deeper layers of the ocean. Actually, acidification and deoxygenation in the JES interior are linked to each other via the remineralization of OM because of increasing nutrient concentrations, NDIC, and decreasing DO and pH over time, as was observed before [46]. Using Redfield

stoichiometry [47] for OM, the process of aerobic respiration can be formally represented by the following scheme:



The main conclusion from our results is that a remineralization of OM (Equation (5)) in the interior of the JES is not a steady-state process.

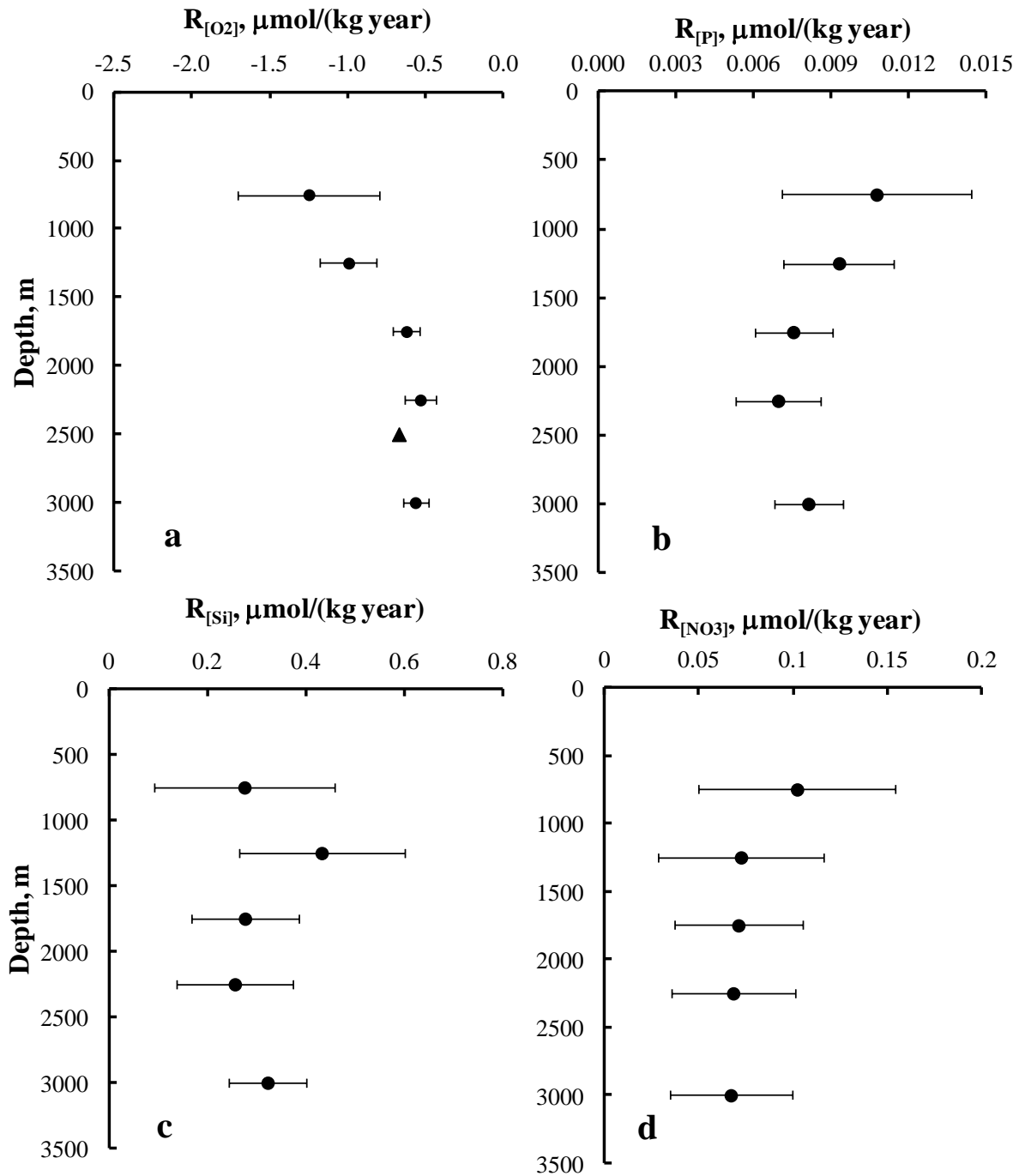


Figure 9. Rates of temporal variability of the averaged hydrochemical parameters in the JES as a function of depth. (a) $R_{[\text{O}_2]}$, $\mu\text{mol}/(\text{kg}\cdot\text{year})$; (b) $R_{[\text{P}]}$, $\mu\text{mol}/(\text{kg}\cdot\text{year})$; (c) $R_{[\text{Si}]}$, $\mu\text{mol}/(\text{kg}\cdot\text{year})$; (d) $R_{[\text{NO}_3]}$, $\mu\text{mol}/(\text{kg}\cdot\text{year})$. The triangle denotes the deoxygenation rate estimated by Gamo et al., 2014 [36]. Bars are 3-s.d. of rates estimated by LSM with the 95% confidence interval.

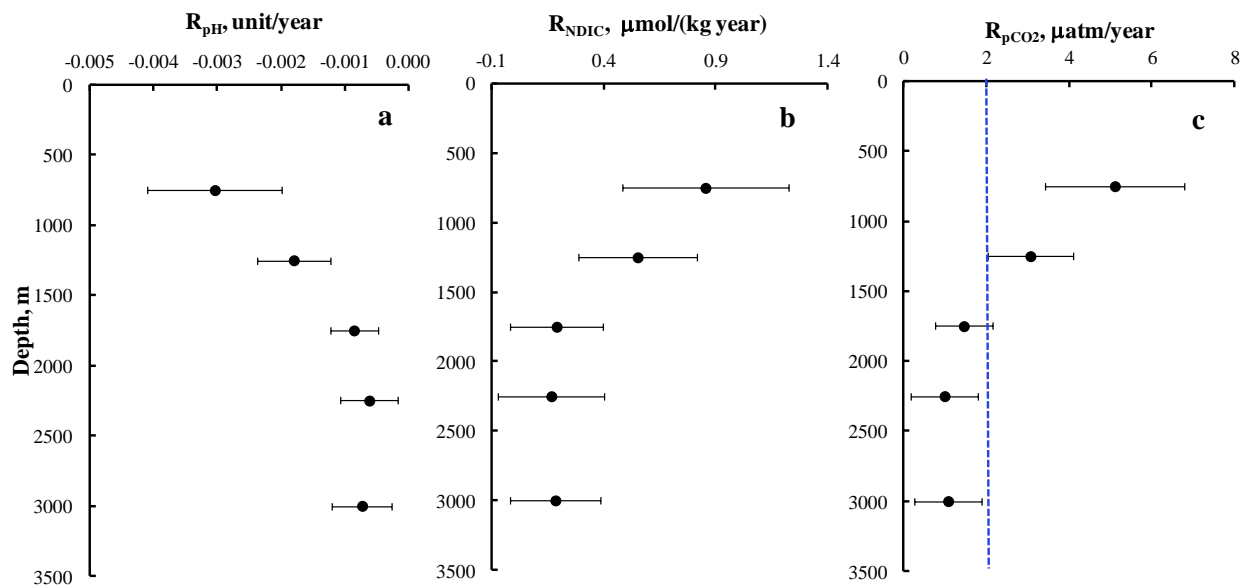


Figure 10. Rates of temporal variability of the averaged carbonate system parameters in the JES as a function of depth. (a) $R_{[pH]}$, pH unit/year; (b) $R_{[NDIC]}$, $\mu\text{mol}/(\text{kg}\cdot\text{year})$; (c) $-R_{[pCO_2]}$, $\mu\text{atm}/\text{year}$. Bars are 3-s.d. of rates estimated by LSM with the 95% confidence interval. The dashed line shows the rate of expected changes based on atmospheric CO_2 alone.

There are three possible explanations (hypotheses) for the obtained findings. It should be noted that all of them have been considered by Gamo et al. [3] regarding the decrease in DO concentration in the bottom water in the JES: “The temporal decrease of oxygen concentration is, therefore, thought to reflect either of the three possibilities: the reduction or cessation of the supply of the new bottom water, the increase of falling organic materials, and the enhancement of vertical mixing between the bottom layer and the deep layer. The third case would result in an increase of oxygen content of the deep layer as expected from the material balance between the deep and bottom layers. Actually, the oxygen of the deep layer has also been decreasing since 1977, as shown in Figure 5, so the third case should be erased. The second possibility seems to be unlikely because there has been no remarkable increase of biological activity as deduced from the records of chlorophyll *a* and phaeophytin concentrations and of wet weight values of plankton in the southeastern Japan Sea surface water for the past several years (Maizuru Marine Observatory, 1977–1984). The first possibility is thought to be appropriate” [3]. Further investigations revealed a decrease in the DO concentration in the water column rather than in certain water masses, as in the case of Yamato Basin [36], which means the third explanation does not work. We fully agree with this conclusion [3] because a comparison of the hydrochemical parameters obtained in 1999 and 2014 demonstrates a shift in concentrations for all water masses of the JES except for the upper 500 m (Figure 11). Finally, the generally accepted explanation for the deoxygenation of the JES [3–11,36] and acidification [14] is a slowdown of ventilation of Lower Japan Sea Proper Water and Bottom water due to global warming.

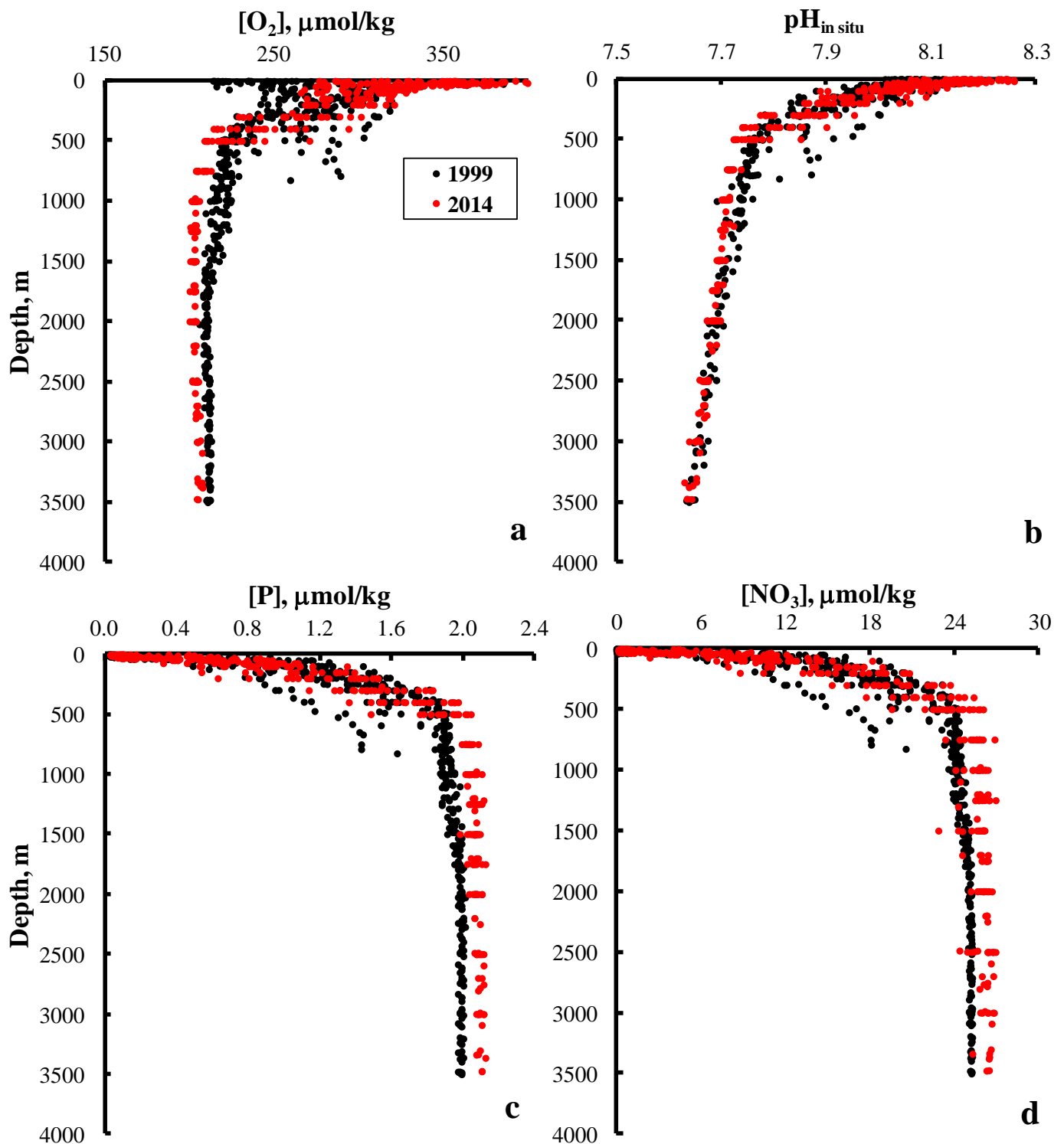


Figure 11. Vertical profiles of measured hydrochemical parameters in the northwestern part of the JES in 1999 (black circles) and 2014 (red circles). (a) DO ($\mu\text{mol/kg}$); (b) $\text{pH}_{\text{in situ}}$; (c) phosphorus concentration ($\mu\text{mol/kg}$); (d) nitrate concentration ($\mu\text{mol/kg}$).

It should be noted that even a decreasing ventilation rate will be the same for different water masses, so the rates of their deoxygenation, acidification, and increase in nutrients would be different in different water masses. This is because the OM produced at the euphotic layer will experience remineralization as it descends. As this OM is oxidized, the amount of OM reaching the deeper layers will be lower [14]. Therefore, the Upper Japan

Sea Proper Water will have a larger increase in nutrients and a larger decrease in pH and DO, as reported before by [14]. If a slowing down of the ventilation of the water column in the JES is responsible for the observed temporal variability in hydrochemical parameters, then reducing the nutrient supply from the interior of the sea into the euphotic layer would be expected. Consequently, that will lead to a reduction in primary production (PP), i.e., an oligotrophication of the JES, because an oligotrophication means “a decrease in the rate of supply of organic matter to an ecosystem” [48]. There is a publication that supports the idea that oligotrophication of the JES has occurred [49]. Because the authors of this publication used satellite ocean color data and an available model, they estimated a decreasing trend (13% per 10 years) in the annual PP in the JES from 2003 to 2012 [49]. However, as noted by Ishizaka et al. [50], the authors of the work [49] have not provided any clues on how the decrease PP was related to the increase of Chl-*a* reported by Lee et al. [51]. We think that the results obtained by Lee et al. [51] indicate an increase in of PP over time.

We do not rule out that a decrease in vertical ventilation plays some role in the unsteady state of remineralization of the OM rate with the depth of the JES (Equation (5)); however, we suggest that a second explanation of the deoxygenation given in [3] also contributed in the northwestern part of the JES, namely the increase in PP over time. In other words, it means eutrophication of the JES [45–48]. First, there is a lot of evidence regarding the eutrophication of the PGB, for example, Figure 9. Increasing PP over time will result in additional exportation of particulate organic matter (POM) from the surface to the deep layers by diatoms insofar as diatoms dominate in the microalgae population of the JES [52]. This hypothesis easily explains the more intensive acidification and deoxygenation at 750 m depth when intense mesoscale water dynamics in the northwestern part of the JES near the 500 m depth occurred (Figure 3; [53]). An increase in PP leads to enhanced exportation of POM to the deeper layers.

There are three possible causes for the increase in PP in the northwestern part of the JES. One is the transport of waters enriched by nutrients. These are shallow waters from the PGB and the East China Sea (ECS) that flow in through the Tsushima (Korea) strait [46,54]. The ECS has a long-term variability in PP due to the eutrophication of its coastal waters [55–57]. However, the impact of eutrophication in the ECS on long-term JES variability is probably limited by the southern part of the JES. The second reason is the increase in CO₂ concentration in the atmosphere, which enhances PP [58,59]. This phenomenon clearly affects the whole ocean, including the JES, when the euphotic layer is enriched by nutrients. This occurs in the northwestern part of the JES at the end February to the beginning March due to the formation of a thick, mixed upper layer [1,2,20]. There is a third regional reason that could be associated with the atmospheric contamination around the JES. Recent observations suggest strong atmospheric contamination by nitrogen dioxide around China, the coastal area of the Republic of Korea and Japan (Figure S8). In this case, the main atmospheric source of the nutrients for eutrophication of the JES is nitrogen dioxide, which is released into the air by burning coal, gasoline, and biofuels. The JES is thought to be an N-limited basin; therefore, the input of nitrogen may increase PP and the export of POM into the interior of the sea. There are direct observations of increasing atmospheric deposition of nutrients in the Northwestern Pacific Ocean [60,61]. Increasing nitrogen concentrations in the euphotic layer of the JES caused by atmospheric precipitation enhance primary productivity, as investigated using physical ecosystem models [62,63]. Satellite ocean color data that agree with the in situ measurements [49] suggest that chlorophyll *a* concentrations in the euphotic layer slightly increased in the JES in 1998–2011 [51].

There is a synchronization between the regional (shelf of the JES—Amursky Bay) and open part of the JES and global biogeochemical processes. Thus, maximal changes in the composition and structure of bottom fauna in the Amursky Bay occurred at the same time in the 1970s–1980s, when the minimum DO values declined to a hypoxic state (Figure 2). We consider the 1970s–1980s as a time of ecological shift on the shelf of the JES. Almost at the same time, a decrease in DO concentrations in the bottom waters of the

open part of the Sea of Japan was documented [3]. This regional deoxygenation of open JES and its shelf coincides with global processes such as an explosive increase in hypoxia events and eutrophication in the coastal oceans, the industrial production of total active nitrogen [64,65], and deoxygenation of the world's oceans [66]. Obviously, there are global processes that promote deoxygenation in coastal and open oceans, such as contamination of the atmosphere by nutrients and global warming [43,60,61,66,67]. Both global processes will make similar contributions to the temporal variability of hydrochemical parameters, namely the increase in nutrients and carbon dioxide concentrations and the decrease in DO concentrations and the pH in the interior of the ocean. It is very difficult to distinguish the impacts of these global processes on the variability of oceans, including the JES. Further efforts are necessary to distinguish drivers that result in the unsteady state of respiration of OM in the interior of the JES.

Supplementary Materials: The following are available online at <https://www.mdpi.com/article/10.3390/jmse9090953/s1>: Figure S1. Ranked nitrite + nitrate results for all samples. Reported concentrations were sorted using the concentration of sample 5; Figure S2. Ranked nitrate results for all samples. Reported concentrations were sorted using the concentration of sample 5; Figure S3. Ranked nitrite results for all samples. Reported concentrations were sorted using concentration of sample 1; Figure S4. Ranked phosphate results for all samples. Reported concentrations were sorted using the concentration of sample 5; Figure S5. Ranked silicate results for all samples. Reported concentrations were sorted using the concentration of sample 5; Figure S6. Vertical distribution of (a) pHT (15 °C)—and (b) dissolved oxygen in the water column. Station CR-02, KH-10-02 cruise, June 2010, Japan/East Sea; Figure S7. Comparison of pH data measured at 15 °C in “total hydrogen concentration scale” for Japan Sea. Black is the Lavretyev cruise in 2009; Red is the Hakuho-Maru 2010, leg1; Green is the Hakuho-Maru 2010, leg 2; Figure S8. Nitrogen dioxide worldwide pollution. (a) NASA's Earth-observing satellite, Aura, measures the air pollutant nitrogen dioxide (NO₂) from high above the Earth's surface. (https://eosps0.gsfc.nasa.gov/sites/default/files/publications/NO2_GlobalLenticular_508.pdf (Figure was accessed on 1 July 2020)); (b) Measurements gathered by the Copernicus Sentinel-5P mission between April and September 2018 have been averaged to reveal nitrogen dioxide in the atmosphere, ESA data. (http://www.esa.int/spaceinimages/Images/2019/03/Nitrogen_dioxide_worldwide (Figure was accessed on 1 July 2020)). Table S1. The average hydrochemical parameters ([DO], [P], [NO₃⁻], [Si], n—number of measurements, s.d.—standard deviation of the mean) of the JES at nominal depths for different years; Table S2. The average carbonate system parameters ([NTA], [pH], [NDIC], pCO₂, n = number of measurements, s.d.—standard deviation of the mean) of the JES at nominal depths for different years.

Author Contributions: Primary writing: P.T. (Pavel Tishchenko) and V.L. Synthesis and overall coordination: V.L., D.K. and P.T. (Pavel Tishchenko). Hydrochemical measurements, data correction and processing/analysis: S.S., P.T. (Pavel Tishchenko), and P.T. (Petr Tishchenko). Estimation of acidification on the shelf: P.T. (Petr Tishchenko) Discussion/revision: P.T. (Pavel Tishchenko), V.L., D.K. and P.T. (Petr Tishchenko). All authors have read and agreed to the published version of the manuscript.

Funding: This study was partly supported by the Russian Foundation for Basic Research (21-55-53015-a) and Fundamental Programs of POI—01201363041 and 01201353055.

Institutional Review Board Statement: The study did not involve humans and animals.

Informed Consent Statement: The study did not involve humans.

Data Availability Statement: All data are available in Supplementary Materials.

Acknowledgments: We would like to thank Kyung-Ryul Kim and Kuh Kim, Dong-Jing Kang, and Kyung Il Chang, and Guebuem Kim, who put much effort into the development of the CREAMS program and organizing joint cruises, and for valuable discussions. Many thanks to all Russian and Korean researchers and students who participated in the joint cruises as well as the captains and crews of R/V *Akademik M.A. Lavrentyev*, Professor *Gagarinskiy*, Professor *Khromov*, and Roger Revelle for their hard work at sea. Special thanks to Lynne Talley for her enthusiastic efforts in organizing CREAMS-II international cruises.

Conflicts of Interest: We declare no competing interest.

References

1. Talley, L.; Min, D.-H.; Lobanov, V.; Luchin, B.A.; Ponomarev, V.I.; Salyuk, A.; Shcherbina, A.; Tishchenko, P.; Zhabin, I. Japan/East Sea Water Masses and their Relation to the Sea's Circulation. *Oceanography* **2006**, *19*, 32–49. [[CrossRef](#)]
2. Talley, L.D.; Lobanov, V.; Ponomarev, V.; Salyuk, A.; Tishchenko, P.; Zhabin, I.; Riser, S. Deep convection and brine rejection in the Japan Sea. *Geophys. Res. Lett.* **2003**, *30*, 1159. [[CrossRef](#)]
3. Gamo, T.; Nozaki, Y.; Sakai, H.; Nakai, T.; Tsubota, H. Spatial and temporal variations of water characteristics in the Japan Sea bottom layers. *J. Mar. Res.* **1986**, *44*, 781–793. [[CrossRef](#)]
4. Kim, K.-R.; Kim, K. What is happening in the East Sea (Japan Sea)?: Recent chemical observations from CREAMS 93–96. *J. Korean Soc. Oceanogr.* **1996**, *31*, 164–172.
5. Kim, K.-R.; Kim, K.; Kang, D.-J.; Park, S.Y.; Park, M.-K.; Kim, Y.-G.; Min, H.-S.; Min, D. The East Sea (Japan Sea) in change: A story of dissolved oxygen. *MTS J.* **1999**, *33*, 15–22. [[CrossRef](#)]
6. Gamo, T. Global warming may have showed down the deep conveyor belt of a marginal sea of the northwestern Pacific: Japan Sea. *Geophys. Res. Lett.* **1999**, *26*, 3137–3140. [[CrossRef](#)]
7. Chen, C.T.A.; Bychkov, A.S.; Wang, S.L.; Pavlova, G.Y. An anoxic Sea of Japan by the year 2200? *Mar. Chem.* **1999**, *67*, 249–265. [[CrossRef](#)]
8. Ponomarev, V.I.; Salyuk, A.N. The climate regime shifts and heat accumulation in the Sea of Japan. In Proceedings of the CREAMS'97 International Symposium, Fukuoka, Japan, 28–30 January 1997; pp. 157–161.
9. Kim, K.; Kim, K.-R.; Min, D.-H.; Volkov, Y.; Yoon, J.-H.; Takematsu, M. Warming and structural changes in the East (Japan) Sea: A clue to future changes in global oceans? *Geophys. Res. Lett.* **2001**, *28*, 3293–3296. [[CrossRef](#)]
10. Kang, D.-J.; Kim, J.-Y.; Lee, T.; Kim, K.-R. Will the East/Japan Sea become an anoxic sea in the next century? *Mar. Chem.* **2004**, *91*, 77–84. [[CrossRef](#)]
11. Kim, K.; Kim, K.-R.; Kim, Y.-G.; Cho, Y.-K.; Kang, D.-J.; Takematsu, M.; Volkov, Y. Water mass and decadal variability in the East Sea (Sea of Japan). *Prog. Oceanogr.* **2004**, *61*, 157–174. [[CrossRef](#)]
12. Kim, T.-W.; Lee, K.; Feely, R.A.; Sabine, C.L.; Chen, C.-T.A.; Jeong, H.J.; Kim, K.Y. Prediction of Sea of Japan (East Sea) acidification over the past 40 years using a multiparameter regression model. *Glob. Biogeochem. Cycles* **2010**, *24*, GB3005. [[CrossRef](#)]
13. Kim, J.-Y.; Kang, D.-J.; Lee, T.; Kim, K.-R. Long-term trend of CO₂ and ocean acidification in the surface water of the Ulleung Basin, the East/Japan Sea inferred from the underway observational data. *Biogeosciences* **2014**, *11*, 2443–2454. [[CrossRef](#)]
14. Chen, C.-T.A.; Lui, H.-K.; Hsieh, C.-H.; Yanagi, T.; Kosugi, N.; Ishii, M.; Gong, G.-C. Deep oceans may acidify faster than anticipated due to global warming. *Nat. Clim. Chang.* **2017**, *7*, 890–894. [[CrossRef](#)]
15. Tishchenko, P.Y.; Tishchenko, P.P.; Lobanov, V.B.; Mikhaylik, T.A.; Sergeev, A.F.; Semkin, P.Y.; Shvetsova, M.G. Impact of the transboundary Razdolnaya and Tumannaya Rivers on deoxygenation of the Peter the Great Bay (Sea of Japan). *Estuar. Coast. Shelf Sci.* **2020**, *239*, 106731. [[CrossRef](#)]
16. Tishchenko, P.Y.; Lobanov, V.B.; Zvalinsky, V.I.; Sergeev, A.F.; Koltunov, A.; Mikhailik, T.A.; Tishchenko, P.P.; Shvetsova, M.G.; Sagalaev, S.; Volkova, T.I. Seasonal Hypoxia of Amursky Bay in the Japan Sea: Formation and Destruction. *Terr. Atmos. Ocean. Sci.* **2013**, *24*, 1033–1050. [[CrossRef](#)]
17. Tishchenko, P.P.; Tishchenko, P.Y.; Lobanov, V.B.; Sergeev, A.F.; Semkin, P.Y.; Zvalinsky, V.I. Summertime in situ monitoring of oxygen depletion in Amursky Bay (Japan/East Sea). *Cont. Shelf Res.* **2016**, *118*, 77–87. [[CrossRef](#)]
18. Tishchenko, P.Y.; Sergeev, A.F.; Lobanov, V.B.; Zvalinsky, V.I.; Koltunov, A.M.; Mikhajlik, T.A.; Tishchenko, P.P.; Shvetsova, M.G. Hypoxia in near-bottom waters of the Amursky Bay. *Bull. Far East. Branch Russ. Acad. Sci.* **2008**, *6*, 115–125.
19. Mikhaylik, T.A.; Nedashkovsky, A.P.; Khodorenko, N.D.; Tishchenko, P.Y. Peculiarities of the eutrophication of the Amur Bay (Japan Sea) by Razdolnaya River. *Izvetiya TINRO* **2020**, *200*, 401–411. (In Russian) [[CrossRef](#)]
20. Tishchenko, P.Y.; Talley, L.D.; Lobanov, V.B.; Zhabin, I.A.; Luchin, V.A.; Nedashkovskii, A.P.; Sagalaev, S.G.; Chichkin, R.V.; Shkirnikova, E.M.; Ponomarev, V.I.; et al. Seasonal Variability of the hydrochemical conditions in the Sea of Japan. *Oceanology* **2003**, *43*, 643–655.
21. Talley, L.D.; Tishchenko, P.; Luchin, V.; Nedashkovskiy, A.; Sagalaev, S.; Kang, D.-J.; Warner, W.; Min, D.-H. Atlas of Japan (East) Sea hydrographic properties in summer, 1999. *Prog. Oceanogr.* **2004**, *61*, 277–348. [[CrossRef](#)]
22. Hansen, H.P.; Koroleff, F. Determination of nutrients. In *Methods of Seawater Analysis*, 3rd ed.; Grasshoff, K., Kremling, K., Ehrhardt, M., Eds.; Willey-VCH: Weinheim, Germany; New York, NY, USA; Chichester, UK; Brisbane, Australia; Singapore; Toronto, ON, Canada, 1999; pp. 159–251.
23. Tishchenko, P.Y.; Kang, D.-J.; Chichkin, R.V.; Lazaruk, A.Y.; Wong, C.S.; Johnson, W.K. Application of potentiometric method using a cell without liquid junction to underway pH measurements in surface seawater. *Deep Sea Res. Part I* **2011**, *58*, 778–786. [[CrossRef](#)]
24. Dickson, A.G. pH scales and proton-transfer reactions in saline media such as sea water. *Geochim. Cosmochim. Acta* **1984**, *48*, 2299–2308. [[CrossRef](#)]
25. Cai, W.-J.; Hu, X.; Huang, W.-J.; Murrell, M.C.; Lehrter, J.C.; Lohrenz, S.E.; Chou, W.-C.; Zhai, W.; Hollibaugh, J.T.; Wang, Y.; et al. Acidification of subsurface coastal waters enhanced by eutrophication. *Nat. Geosci.* **2011**, *4*, 766–770. [[CrossRef](#)]

26. Zhai, W.D.; Zhao, H.D.; Zheng, N.; Xu, Y. Coastal acidification in summer bottom oxygen-depleted waters in northwestern-northern Bohai Sea from June to August in 2011. *Chin. Sci. Bull.* **2012**, *57*, 1062–1068. [CrossRef]
27. Stunzhas, P.A.; Tishchenko, P.Y.; Ivin, V.V.; Barabanshchikov, Y.A.; Volkova, T.I.; Vishkvartcev, D.I.; Zvalinsky, V.I.; Mikhailik, T.A.; Semkin, P.J.; Tishchenko, P.P.; et al. The First Case of Anoxia in Waters of the Far East Marine Biosphere Reserve. *Dokl. Earth Sci.* **2016**, *467 Pt 1*, 295–298. [CrossRef]
28. Shulkin, V.; Tishchenko, P.; Semkin, P.; Shvetsova, M. Influence of river discharge and phytoplankton on the distribution of nutrients and trace metals in Razdolnaya River estuary, Russia. *Estuar. Coast. Shelf Sci.* **2018**, *211*, 166–176. [CrossRef]
29. Tishchenko, P.Y.; Semkin, P.Y.; Pavlova, G.Y.; Tishchenko, P.P.; Lobanov, V.B.; Marjash, A.A.; Mikhailik, T.A.; Sagalaev, S.G.; Sergeev, A.F.; Tibenko, E.Y.; et al. Hydrochemistry of the Tumen River Estuary, Sea of Japan. *Oceanology* **2018**, *58*, 175–186. [CrossRef]
30. REGIONAL OVERVIEW on River and Direct Inputs of Contaminants into the Marine and Coastal Environment in NOWPAP Region. With Special Focus on the Land Based Sources of Pollution. NOWPAP POMRAC, Vladivostok. 2009. Available online: http://www.pomrac.tigdvo.ru/Pub/DOC/PUBL/POMRAC_RDI_2009.pdf (accessed on 25 August 2021).
31. Tkalin, A.V.; Belan, T.A.; Shapovalov, E.N. The state of marine environment near Vladivostok, Russia. *Mar. Pollut. Bull.* **1993**, *26*, 418–422. [CrossRef]
32. Belan, T.A. Benthos abundance pattern and species composition in conditions of pollution in Amursky Bay (Peter the Great Bay, Sea of Japan). *Mar. Pollut. Bull.* **2003**, *46*, 1111–1119. [CrossRef]
33. Oleinik, E.V.; Moshchenko, A.V.; Lishavskaya, T.S. Impact of Polluted Bottom Deposits on the Species Structure and Abundance of Bivalves in Peter the Great Bay, Sea of Japan. *Russ. J. Mar. Biol.* **2004**, *30*, 20–27. [CrossRef]
34. Silina, A.V.; Ovsyannikova, I.I. Long-term changes in a community of Japanese scallop and its epibionts in the polluted area of Amurskii Bay, Sea of Japan. *Russ. J. Mar. Biol.* **1995**, *21*, 54–60.
35. Sudo, H. A note on the Japan Sea Proper Water. *Prog. Oceanogr.* **1986**, *17*, 313–336. [CrossRef]
36. Gamo, T.; Nakayama, N.; Takahata, N.; Sano, Y.; Zhang, J.; Yamazaki, E.; Taniyasu, S.; Yamashita, N. The Sea of Japan and its Unique Chemistry Revealed by Time-series Observations over the Last 30 years. *Monogr. Environ. Earth Planets* **2014**, *2*, 1–22. [CrossRef]
37. Dore, J.E.; Lukas, R.; Sadler, D.W.; Church, M.J.; Karl, D.M. Physical and biochemical modulation of ocean acidification in the central North Pacific. *Proc. Natl. Acad. Sci. USA* **2009**, *106*, 12235–12240. [CrossRef]
38. Midorikawa, T.; Midorikawa, T.; Ishii, M.; Saito, S.; Sasano, D.; Kosugi, D.; Motoi, T.; Kamiya, H.; Nakadate, A.; Nemoto, K.; et al. Decreasing pH trend estimated from 25-yr time series of carbonate parameters in the western North Pacific. *Tellus* **2010**, *62B*, 649–659. [CrossRef]
39. Byrne, B.H.; Mecking, S.; Feely, R.A.; Liu, X. Direct observations of basin-wide acidification of the North Pacific. *Geophys. Res. Lett.* **2010**, *37*, L02601. [CrossRef]
40. Gonzalez-Davila, M.; Santano-Casiano, J.M.; Rueda, M.J.; Llinas, O. The water column distribution of carbonate system variables at the ESTOC site from 1995 to 2004. *Biogeosciences* **2010**, *7*, 3067–3081. [CrossRef]
41. Bates, N.R.; Best, M.H.P.; Neely, K.; Garley, R.; Dickson, A.G.; Johnson, R.J. Detecting anthropogenic carbon dioxide uptake and ocean acidification in the North Atlantic Ocean. *Biogeosciences* **2012**, *9*, 2509–2522. [CrossRef]
42. Olafsson, J.; Olafsdottir, S.R.; Benoit-Cattin, A.; Danielsen, M.; Arnarson, T.S.; Takahashi, T. Rate of Iceland Sea acidification from time series measurements. *Biogeosciences* **2012**, *6*, 2661–2668. [CrossRef]
43. Doney, S.C. The Growing Human Footprint on Coastal and Open-Ocean Biogeochemistry. *Science* **2010**, *328*, 1512–1516. [CrossRef] [PubMed]
44. Feely, R.A.; Sabine, C.L.; Lee, K.; Berelson, W.; Kleypas, J.; Fabry, V.J.; Millero, F.J. Impact of Anthropogenic CO₂ on the CaCO₃ System in the Oceans. *Science* **2004**, *305*, 362–366. [CrossRef]
45. Duarte, C.M.; Hendriks, I.E.; Moore, T.S.; Olsen, Y.S.; Steckbauer, A.; Ramajo, L.; Carstensen, J.; Trotter, J.A.; McCulloch, M. Is Ocean Acidification an Open-Ocean Syndrome? Understanding Anthropogenic Impacts on Seawater pH. *Estuaries Coasts* **2013**, *36*, 221–236. [CrossRef]
46. Tishchenko, P.Y.; Talley, L.D.; Nedashkovsky, A.P.; Sagalaev, S.G.; Zvalinsky, V.I. Temporal Variability of the Hydrochemical Properties of the Waters of the Sea of Japan. *Oceanology* **2002**, *42*, 795–803.
47. Redfield, A.C.; Ketchum, B.H.; Richards, F.A. The influence of organisms on the composition of sea-water. In *The Composition of Seawater: Comparative and Descriptive Oceanography*; Hill, M.N., Ed.; The Sea Interscience: New York, NY, USA, 1963; Volume 2, pp. 26–77.
48. Nixon, S.F. Eutrophication and macroalgae. *Hydrobiologia* **2009**, *629*, 5–19. [CrossRef]
49. Joo, H.-T.; Son, S.H.; Park, J.W.; Kang, J.J.; Jeong, J.-Y.; Lee, J.I.; Kang, C.-K.; Lee, S.H. Long-Term Pattern of Primary Productivity in the East/Japan Sea Based on Ocean Color Data Derived from MODIS-Aqua. *Remote Sens.* **2016**, *8*, 25. [CrossRef]
50. Ishizaka, J.; Yamada, K. Phytoplankton and Primary Production in the Japan Sea. In *Remote Sensing of the Asian Seas*; Barale, V., Gade, M., Eds.; Springer: Cham, Switzerland, 2019; pp. 177–189. [CrossRef]
51. Lee, S.H.; Son, S.; Dahms, H.U.; Park, J.W.; Lim, J.H.; Noh, J.H.; Kwon, J.I.; Joo, H.T.; Jeong, J.Y.; Kang, C.K. Decadal changes of phytoplankton chlorophyll-a in the East Sea/Sea of Japan. *Oceanology* **2014**, *54*, 771–779. [CrossRef]
52. Konovalova, G.V.; Orlova, T.Y.; Pautova, L.A. *Atlas of Phytoplankton of the Sea of Japan*; Nauka: Leningrad, Russia, 1989; p. 160. (In Russian)

53. Lobanov, V.B.; Ponomarev, V.I.; Salyuk, A.N.; Tishchenko, P.Y.; Talley, L.D. Structure and dynamics of synoptic scale eddies in the northern Japan Sea. In *Far Eastern Seas of Russia; Oceanographic Research*; Nauka: Moscow, Russia, 2007; Volume 1, pp. 450–473. (In Russian)
54. Andreev, A.G. Interannual Variations of Sea Water Parameters and Chlorophyll *a* Concentration in the Japan Sea in Autumn. *Russ. Meteorol. Hydrol.* **2014**, *39*, 542–549. [[CrossRef](#)]
55. Yoo, S.; An, Y.-R.; Bae, S.; Choi, S.; Ishizaka, J.; Kang, Y.-S.; Kim, Z.G.; Lee, C.; Lee, J.B.; Li, R.; et al. Status and trends in the Yellow Sea and East China Sea region. In *Marine Ecosystems of the North Pacific Ocean, 2003–2008*; McKinnell, S.M., Dagg, M.J., Eds.; PICES Special Publication: Sidney, BC, Canada, 2010; Volume 4, pp. 360–393.
56. Ning, X.; Lin, C.; Su, J.; Liu, C.; Hao, Q.; Leet, F. Long-term changes of dissolved oxygen, hypoxia, and the responses of the ecosystems in the East China Sea from 1975 to 1995. *J. Oceanogr.* **2011**, *67*, 59–75. [[CrossRef](#)]
57. Wang, B.; Xin, M.; Wei, Q.; Xie, L. A historical overview of coastal eutrophication in the China Seas. *Mar. Pollut. Bull.* **2018**, *136*, 394–400. [[CrossRef](#)] [[PubMed](#)]
58. Hein, M.; Sand-Jensen, K. CO₂ increases oceanic primary production. *Nature* **1997**, *388*, 526–527. [[CrossRef](#)]
59. Riebesell, U.; Schulz, K.G.; Bellerby, R.G.J.; Botros, M.; Fritsche, P.; Meyerhöfer, M.; Neill, C.; Nondal, G.; Oschlies, A.; Wohlers, J.; et al. Enhanced biological carbon consumption in a high CO₂ ocean. *Nature* **2007**, *450*, 545–549. [[CrossRef](#)]
60. Kim, T.-W.; Lee, K.; Najjar, R.G.; Jeong, H.-D.; Jeong, H.J. Increasing N Abundance in the Northwestern Pacific Ocean Due to Atmospheric Nitrogen Deposition. *Science* **2011**, *334*, 505–508. [[CrossRef](#)]
61. Kim, I.-N.; Lee, K.; Gruber, N.; Karl, D.M.; Bullister, J.L.; Yang, S.; Kim, T.-W. Increasing anthropogenic nitrogen in the North Pacific Ocean. *Science* **2014**, *346*, 1102–1106. [[CrossRef](#)] [[PubMed](#)]
62. Onitsuka, G.; Uno, I.; Yana, T.; Yoon, J.-H. Modeling the Effects of Atmospheric Nitrogen Input on Biological Production in the Japan Sea. *J. Oceanogr.* **2009**, *65*, 433–438. [[CrossRef](#)]
63. Lee, S.; Yoo, S. Interannual variability of the phytoplankton community by the changes in vertical mixing and atmospheric deposition in the Ulleung Basin, East Sea: A modelling study. *Ecol. Model.* **2016**, *322*, 31–47. [[CrossRef](#)]
64. Boesch, D.F. Challenges and Opportunities for Science in Reducing Nutrient Over-enrichment of Coastal Ecosystems. *Estuaries* **2002**, *25*, 886–900. [[CrossRef](#)]
65. Rabalais, N.N.; Diaz, R.J.; Levin, L.A.; Turner, R.E.; Gilbert, D.; Zhang, J. Dynamics and distribution of natural and human-caused hypoxia. *Biogeosciences* **2010**, *7*, 585–619. [[CrossRef](#)]
66. Schmodtke, S.; Stramma, L.; Visbeck, M. Decline in global oceanic oxygen content during the past five decades. *Nature* **2017**, *542*, 335–339. [[CrossRef](#)]
67. Breitburg, D.; Levin, L.A.; Oschlies, A.; Gregoire, M.; Chavez, F.P.; Conley, D.J.; Garçon, V.; Gilbert, D.; Gutierrez, D.; Isensee, K.; et al. Declining oxygen in the global and coastal waters. *Science* **2018**, *359*, eaam7240. [[CrossRef](#)]